

# Regulating Cyan Fluorescent Triangular Molecules to Emit White Light in Solution and Gel Based on an Artificial Light-Harvesting System

Xinxian Ma,<sup>\*,∇</sup> Yuehua Liang,<sup>∇</sup> Jiuzhi Wei, Juan Zhang, Enke Feng, Zhenxing Fu, Shixun Lian,<sup>\*</sup> and Yun Yan<sup>\*</sup>



Cite This: *ACS Appl. Opt. Mater.* 2024, 2, 1903–1910



Read Online

ACCESS |



Metrics & More



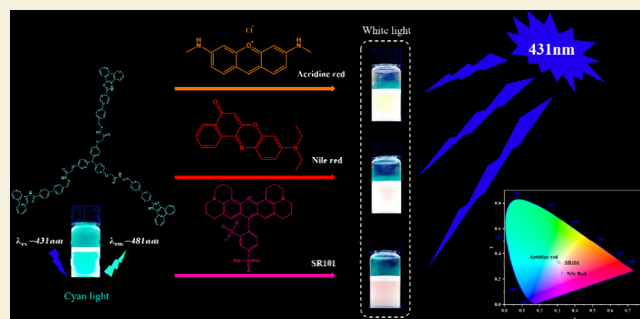
Article Recommendations



Supporting Information

**ABSTRACT:** Inspired by Förster resonance energy transfer (FRET) and natural photosynthetic systems, we report a triangular molecule of phenanthroimidazole Schiff base (T), verifying through time-dependent density functional theory calculations that molecule T can undergo FRET with red fluorescent dyes. Subsequent experiments confirmed that it can be used to construct three artificial light harvesting systems through FRET with Nile Red, Acridine Red, and SR101, and all of them have successfully achieved tunable fluorescence of white light emission. At the same time, the molecule was prone to react with alkaline substances, leading to deprotonation and quenching of its fluorescence. This made the DMSO solution of molecule T suitable as an alkaline gas detection material. Finally, a multiperformance gel composed of PVA and molecular T was prepared and applied to information writing materials. It is worth noting that this is the first report on white light emitted by phenanthroimidazole derivatives through the FRET effect.

**KEYWORDS:** FRET, white light material, phenanthroimidazole, gel, TD-DFT



## INTRODUCTION

Photosynthesis is a process where green plants and certain bacteria convert light energy into chemical energy, playing a crucial role in the ecosystem.<sup>1,2</sup> Inspired by photosynthesis, artificial light-harvesting systems (ALHSs) have been developed to achieve the efficient capture of light energy. The implementation of white light regulation in constructing ALHSs can improve the utilization and conversion of light energy, providing new avenues for the generation of renewable energy. In recent years, a large number of ALHSs have been constructed, including supermolecular fluorescent hydrogels,<sup>3,4</sup> dry gels,<sup>5</sup> polymers,<sup>6,7</sup> organic/inorganic supermolecular coassembled hydrogels,<sup>8,9</sup> micelles,<sup>10–12</sup> supermolecular self-assembled materials,<sup>13–16</sup> nanocrystals,<sup>17,18</sup> and complexes.<sup>19,20</sup>

At the same time, there are increasing reports on white light ALHSs. For example, Bairi and colleagues mixed melanine (M), 6,7-dimethoxy-2,4[1H,3H]-quinazolinedione (Q), riboflavin (R), and rhodamine B (RhB). According to the ratio of M:Q:R:RhB = 100:100:0.5:0.02 to generate white light hydrogel (W-gel), the color coordinate of the gel is (0.31, 0.36).<sup>21</sup> Xiao and colleagues reported ALHSs composed of secondary energy transfer effects, which exhibit white light emission at a ratio of M/ESY/NDI = 1000/5/1, with color

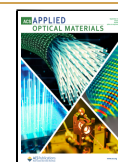
coordinates of (0.31, 0.33).<sup>22</sup> It is worth noting that the multicomponent construction of white light systems has the disadvantage of difficult proportion control and the need to consider the properties of each component in practical applications. This makes the two-component construction of white light ALHSs easy to apply. Tong et al. reported a series of fluorescent materials derived from phenanthrimidazole, demonstrating that by increasing the length of the conjugated bridge in phenanthrimidazole, the fluorescence of the compound could shift from dark blue to blue light.<sup>23</sup> This provided us with the idea of using two components of blue and red light to form white light ALHSs. Based on this, we designed a three-arm molecule of the phenanthroimidazole–acylhydrazone (molecule T). The fluorescence emission spectrum of molecule T substantially overlapped with the fluorescence absorption spectra of red light emitting such as Nile Red, SR101, and Acridine Red. Thus, fluorescence

**Received:** May 13, 2024

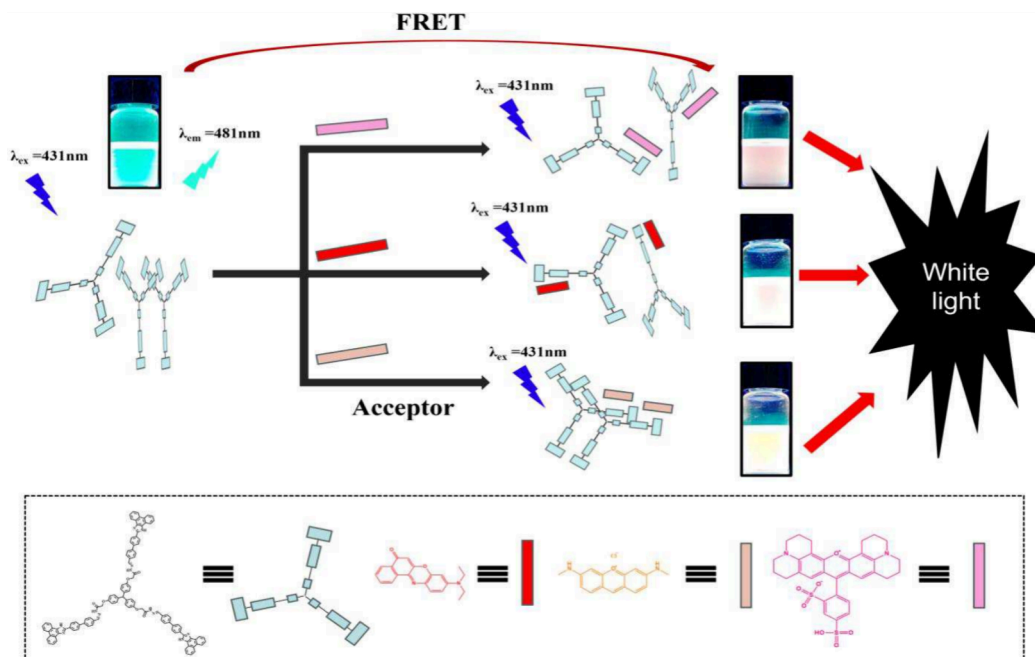
**Revised:** August 13, 2024

**Accepted:** August 14, 2024

**Published:** August 21, 2024



Scheme 1. Schematic Diagram of the Prepared Light-Harvesting Systems



resonance energy transfer (FRET) technology can be used to construct ALHSs, and white light emission can be achieved based on optical complementary cyan light mixed with red light (Scheme 1).<sup>24–26</sup> The data obtained from subsequent synthesis and experimental characterization are very similar to the results calculated using the Gaussian 09 program, proving that molecule T can be modulated using the light-capture system to achieve white light emission. Subsequently, ALHSs were constructed by adding receptors Acridine Red, Nile Red, and SR101, and the occurrence of energy transfer was confirmed by comparing fluorescence spectrograms.<sup>27,28</sup> Finally, three white-light-emitting gels and one cyan-light-emitting gel were prepared, which exhibited high tensile strength and thermoplastic and information storage, offering substantial application potential.

## EXPERIMENTAL SECTION

### Materials and General Methods

Poly(vinyl alcohol) (PVA, polymerization degree 1799, 98–99% alcoholysis) was purchased from Energy Chemical; leucoaurin, ethyl chloroacetate, hydrazine hydrate, potassium carbonate, potassium iodide, *p*-toluenesulfonic acid, acetic acid, ammonium acetate, DMF, SR101, 9,10-phenanthraquinone, 4,4'-biph-enydicarbaldehyde, DMSO, Acridine Red, Nile Red, metal salts, aqueous ammonia, pyridine, triethylamine, diethylamine, oleylamine, sulfuric acid, and triethanolamine were purchased from Sinopharm Chemical Reagent Co., Ltd.

All of the above compounds were used directly without further purification. Distilled water was used for all of the experiments.

<sup>1</sup>H NMR (400 MHz) and <sup>13</sup>C NMR spectra (101 MHz) were carried out with a Bruker 400 MHz spectrometer. Fluorescence spectra were measured on a Shimadzu RF-6000 fluorescence spectrophotometer. The quantum yields (QYs) were obtained by employing the Edinburgh FLS1000 instrument. The ultraviolet–visible (UV–vis) absorption spectra of the samples were recorded by a Shimadzu UV-1750 spectrometer. The hand-held illuminometer is used to test the illuminance of fluorescence emitted by the gel after being excited by ultraviolet light. The fluorescence lifetimes were recorded on a time-correlated single-photon counting spectrometer

(Edinburgh FLS1000). The quantum chemistry calculation was performed at the PBE0/6-311G\* level of theory by using the TD-DFT method in the Gaussian 09 software.

### Synthesis of Compounds

The detailed synthesis process can be found in Scheme S1.

**Synthesis of Compound 1.** 4,4',4''-Methylenetriphenol (5.00 g, 17.10 mmol) was dissolved in *N,N*-dimethylformamide (DMF, 50 mL). Then potassium carbonate (7.09 g, 51.31 mmol), potassium iodide (0.30 g, 1.80 mmol), and ethyl chloroacetate (6.39 g, 52.16 mmol) were added. The mixture was stirred for 12 h at 100 °C. Then hydrazine hydrate (12.83 g, 0.26 mol) was added, stirred at 80 °C for 10 h, and washed four times by filtration with water. After the product was dried in a vacuum, a gray solid was obtained (6.69 g, yield: 76.96%). <sup>1</sup>H NMR (400 MHz, DMSO-*d*<sub>6</sub>, Figure S4)  $\delta$  (ppm): 9.32 (s, 3H), 6.98 (d, *J* = 8.4 Hz, 6H), 6.87 (d, *J* = 8.6 Hz, 6H), 5.42 (s, 1H), 4.44 (s, 6H), 4.33 (s, 6H). <sup>13</sup>C NMR (101 MHz, DMSO-*d*<sub>6</sub>, Figure S5)  $\delta$  (ppm): 167.14, 156.54, 137.47, 130.24, 114.87, 114.58, 66.68, 53.80.

**Synthesis of Compound 2.** 9,10-Phenanthraquinone (4.00 g, 19.21 mmol), ammonium acetate (12.00 g, 0.16 mol), and biphenyl dialdehyde (4.04 g, 19.22 mmol) were dissolved in 60 mL of acetic acid, and the mixture was stirred at 130 °C for 8 h and washed four times by filtration with water. After the product was dried in vacuum, a yellow powder was obtained (6.49 g, yield: 80.76%). <sup>1</sup>H NMR (400 MHz, DMSO-*d*<sub>6</sub>, Figure S6)  $\delta$  (ppm): 13.61 (s, 1H), 10.09 (d, *J* = 1.9 Hz, 1H), 8.88 (d, *J* = 8.2 Hz, 2H), 8.60 (d, *J* = 8.0 Hz, 2H), 8.47 (d, *J* = 8.1 Hz, 2H), 8.06 (d, *J* = 8.0 Hz, 6H), 7.76 (t, *J* = 7.4 Hz, 2H), 7.66 (t, *J* = 7.7 Hz, 2H). <sup>13</sup>C NMR (101 MHz, DMSO-*d*<sub>6</sub>, Figure S7)  $\delta$  (ppm): 193.28, 193.22, 149.05, 145.46, 139.48, 136.23, 135.71, 130.94, 130.69, 130.65, 128.37, 128.15, 128.11, 127.74, 127.63, 127.55, 127.22, 125.82, 124.42, 122.50.

**Synthesis of Compound T.** Compound 2 (2.00 g, 5.02 mmol) was dissolved in *N,N*-dimethylformamide (DMF, 20 mL), then *p*-methylbenzenesulfonic acid (0.02 g, 0.11 mmol) was added and compound 1 (0.85 g, 1.67 mmol) was added after stirring for 10 min. The mixture was stirred at 75 °C for 7 h and filtered four times with water. After the product was dried in a vacuum, a yellow powder was obtained with molecular T (2.41 g, yield: 84.56%). <sup>1</sup>H NMR (400 MHz, DMSO-*d*<sub>6</sub>, Figure S8)  $\delta$  (ppm): 13.55 (d, *J* = 16.4 Hz, 3H), 11.64 (d, *J* = 9.2 Hz, 3H), 8.92–8.82 (m, 6H), 8.60 (dt, *J* = 19.6, 5.6 Hz, 6H), 8.45 (ddd, *J* = 19.5, 9.1, 4.8 Hz, 7H), 8.11–8.04 (m, 4H),

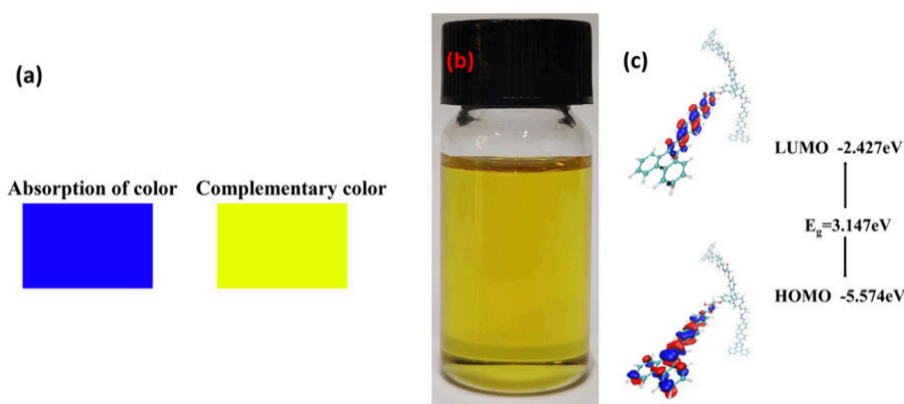


**Figure 1.** (a) Excitation energies of the lowest 50 states of the molecule T in a DMSO solution were calculated using the Gaussian 09 program; the resulting data were plotted using the Multiwfn program to obtain the absorption spectrum and complementary color map of molecule T in the DMSO solvent. (b) Molecule T in DMSO was photographed under natural light ( $[T] = 1 \times 10^{-2}$  mol/L). (c) Calculated highest occupied molecular orbital and lowest unoccupied molecular orbital plots of molecule T.

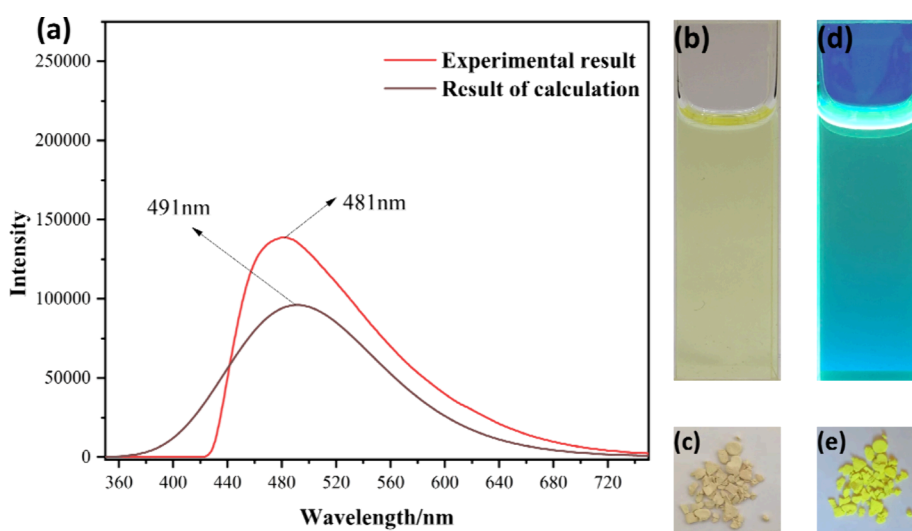


**Figure 2.** (a) Fluorescence emission spectra of molecule T in DMSO ( $[T] = 10^{-3}$  mol/L,  $\lambda_{\text{ex}} = 431$  nm) calculated using the Gaussian 09 program. (b and c) Photographs of the DMSO solution and solid powder of molecule T under natural light. Parts (d) and (e) correspond to (b) and (c), respectively, under UV irradiation (365 nm) ( $[T] = 10^{-3}$  mol/L).

8.01–7.94 (m, 5H), 7.86 (dd,  $J = 19.9, 7.8$  Hz, 10H), 7.75 (d,  $J = 9.9$  Hz, 7H), 7.65 (t,  $J = 7.3$  Hz, 6H), 7.08–6.86 (m, 12H), 5.16 (s, 3H), 4.67 (s, 3H).  $^{13}\text{C}$  NMR (101 MHz, DMSO- $d_6$ , Figure S9)  $\delta$  (ppm): 169.61, 164.85, 156.98, 156.52, 149.14, 147.91, 143.82, 140.98, 140.14, 137.62, 133.84, 130.69, 130.25, 128.28, 128.13, 128.06, 127.59, 127.41, 127.18, 125.81, 124.59, 124.26, 122.84, 122.47, 114.96, 114.78, 65.22. EI-MS (Figure S11)  $m/z$ :  $[M + \text{Na}]^+$  calcd, 1671.59; found, 1672.1609.

## RESULTS AND DISCUSSION

After designing the synthesis process of molecule T (Scheme S1), we performed time-dependent density functional theory (TD-DFT) calculations to predict the fluorescence spectrum of molecule T and judge whether it has synthetic value. Since all the solvents used in our subsequent experiments are DMSO, we used the method of linear response to calculate, and the DMSO solvent environment was represented using the polarizable continuum model (PCM) solvation model. First, we used the pure functional PBE0 6-311G\* basis set to calculate the geometric structure of the solvent considering ground-state optimization (Figure S1). Second, we calculated the energy of the lowest 50 excited states of molecule T in the

DMSO solution using the Gaussian 09 program. The data were input to the Multiwfn program to determine the color of molecule T dissolved in DMSO.<sup>29,30</sup> The peak intensity of the ultraviolet ray absorption spectrum obtained by experiments was almost the same as that obtained by calculations (Figure S2), and the color of molecule T in DMSO was in the yellow series, consistent with the predictions (Figures 1a and 2b). Then, we obtained the  $S_0 \rightarrow S_1$  excitation energy and corresponding molecular orbital map by optimizing the  $S_1$  excited state structure of molecule T in DMSO (Figure 1c). Subsequently, we plotted the corresponding fluorescence emission spectrum using the Multiwfn program (Figure 2a).

In actual experimental tests, we found that molecule T showed an ACQ (aggregation-caused quenching) effect. The concentration of compound T decreased from  $10^{-2}$  to  $10^{-5}$  mol/L, and the fluorescence intensity gradually increased. This means that within this concentration range, an increase in the concentration of compound T will cause aggregation of T in the solution, leading to the occurrence of the ACQ phenomenon. It can also be seen from Figures 2b and 2d, as well as Figures 2c and 2e, that the fluorescence emitted by the solid powder of compound T under UV irradiation is not as

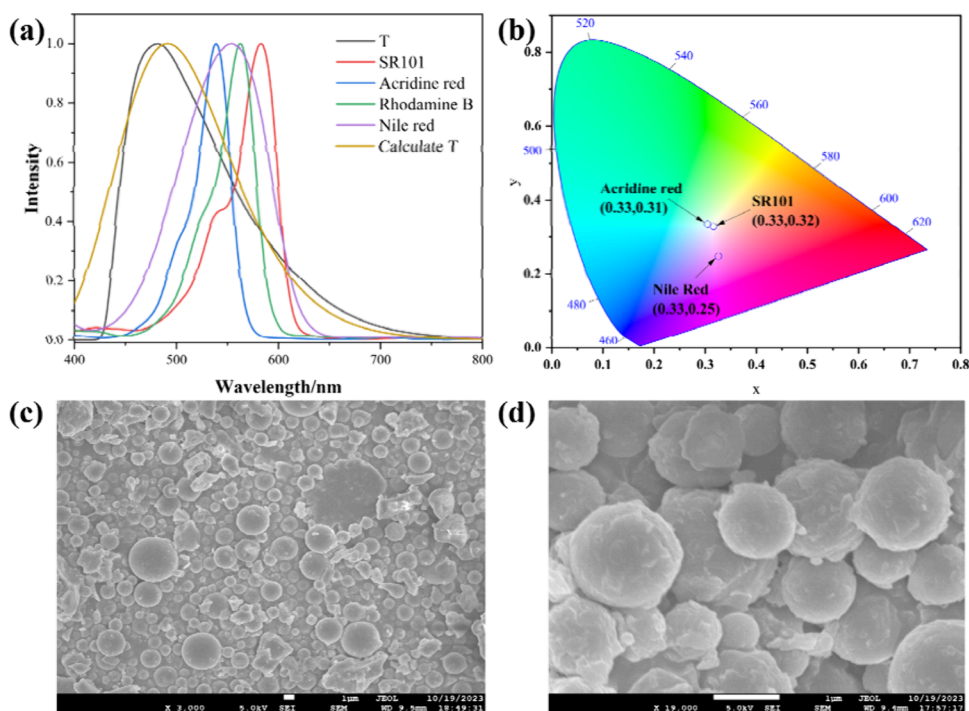


**Figure 3.** (a) Normalized fluorescence absorption spectra of four red fluorescent dyes and the normalized fluorescence emission spectrum of molecule T. (b) White light CIE color gamut diagram of molecule T with SR101, Nile Red, and Acridine Red in molar ratios of 50:1, 20:1, and 20:1, respectively, in a mixed solution ( $[T] = 1 \times 10^{-3}$  mol/L). (c and d) Solid-powder SEM images of molecule T.

strong as that emitted by compound T in DMSO solution. As the concentration further decreases from  $10^{-5}$  to  $10^{-8}$  mol/L, the fluorescence intensity gradually decreases, which is due to the decrease in compound T leading to a decrease in fluorescence intensity (Figure S3). Notably, the wavelength range of the fluorescence emission peak did not change much when the concentration of molecule T changed.

We carefully studied the  $^1\text{H}$  NMR ( $^1\text{H}$  nuclear magnetic resonance) spectra of molecule T with different concentrations, the ground-state structure of molecule T in DMSO using the Gaussian 09 program, and the solid-powder SEM (scanning electron microscope) images of molecule T to understand its ACQ behavior. With increasing concentration, the ground-state structure of molecule T changed from a twisted to planar configuration, the molecular spacing became smaller, and the nonradiative transfer of excited electrons improved, which in turn led to fluorescence quenching. As seen in the SEM image (Figures 3c and 3d), molecule T has been stacked in a spherical shape to achieve the lowest surface energy; this supramolecular structure with tight packing maximized the nonradiative transfer of excited electrons of the nanospheres. As shown in the  $^1\text{H}$  NMR spectrum (Figure S10), with the increase in the concentration, molecule T tended to achieve the planar ground-state structure. Consequently, the intermolecular distance reduced, and peaks corresponding to the benzene ring peaks on the three corners of molecule T merged to form three peaks, peaks corresponding to nitrogen and hydrogen on the imidazole ring and acylhydrazone merged to form a single peak, and the conjugation degree of the central hydrogen with the three benzene rings of another molecule T increased, resulting in an increased shielding effect on the central hydrogen and a decrease in chemical shift. Notably, enhanced fluorescence intensity of molecule T in DMSO was observed at higher or

lower temperatures (Figure S14). At high temperatures, intermolecular vibrations and benzene ring rotation disrupted the tight packing of molecule T. Meanwhile, near the melting point temperature of DMSO, the configuration of molecule T was more inclined toward twisted ground-state configuration with the minimum energy. At the same time, the probability of nonradiative transfer of excited electrons of molecule T decreased with the torsional frequency of the benzene ring, leading to enhanced fluorescence intensity of molecule T.

By comparing the calculated fluorescence emission spectrum of molecule T with the actual fluorescence absorption spectrum of the rhodamine B, SR101, Nile Red, and Acridine Red dye, we reasonably suspected that rhodamine B, SR101, Nile Red, and Acridine Red showed the FRET effect with molecule T based on the overlap range of the fluorescence spectra (Figure 3a). Similarly, their UV spectra also indirectly verified our idea (Figure S12). After considering the calculation results, fluorescence intensity, ACQ effect, and subsequent construction of the light-capture system, we selected a concentration of  $10^{-3}$  mol/L molecule T for subsequent measurements.

Subsequently, the fluorescence excitation emission spectrum was measured at a concentration of  $10^{-3}$  mol/L T molecules in DMSO solution (Figure S13). We added  $10^{-3}$  mol/L molecule T in DMSO solution with rhodamine B, SR101, Nile Red, and Acridine Red for studying the FRET effect and found that only SR101, Nile Red, and Acridine Red exhibited the FRET phenomenon; thus, these three dyes can be used to build a light-capture system. Figure 3b shows the CIE (Commission Internationale de l'Éclairage) color gamut diagram of the white light emission for molecule T with SR101, Nile Red, and Acridine Red with appropriate proportions. After considering the spectral overlap range, actual luminescence intensity, and white light purity, we mainly present the data for Acridine Red

below, and corresponding data for SR101 and Nile Red are included in the SI. As shown in Figure 3a, molecule T in DMSO showed the strongest fluorescence emission peak at 480 nm and the emission band ranges from 420–750 nm. The maximum absorption peak of Acridine Red occurs at 539 nm, and the absorption band is between 440–590 nm in the DMSO solution. Although the degree of overlap between the fluorescence emission spectra of Acridine Red and molecule T is the lowest among the three dyes (Figure 3a), the intensity of white light emitted by the light-capture system formed by Acridine Red and molecule T is the most intense (Figure S15 and Table S1). T–Acridine Red was excited at 431 nm, and white light emitted by the system was captured; the emission color coordinate was calculated to be (0.31, 0.33) (Figure 3b), which was very close to that of the pure white point (0.33, 0.33).

Figure 4a presents the data for a T–Acridine Red based light-capture system. When excited at 431 nm, as Acridine Red

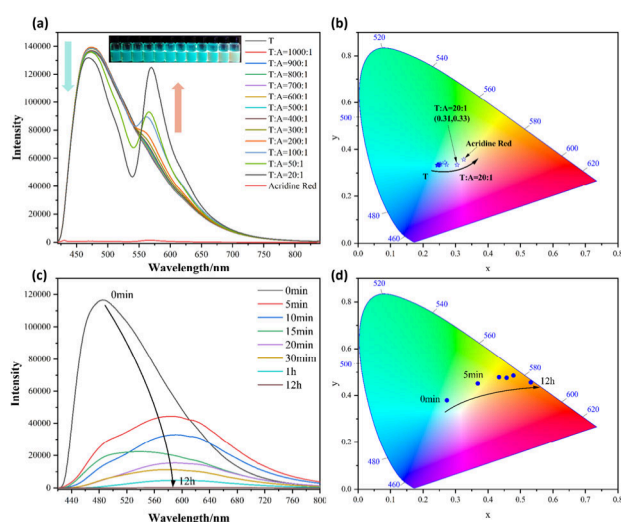


**Figure 4.** (a) Fluorescence emission spectra of molecule T/Acridine Red with different molar amounts of Acridine Red in DMSO. Inset: photographs of the dyes corresponding to the change in molar amount of molecule T/Acridine Red from 1000:1 to 20:1 irradiated with UV light ( $[T] = 5 \times 10^{-4}$  mol/L). (b) CIE gamut diagram corresponding to (a). (c) Fluorescence spectra of molecule T ( $10^{-3}$  mol/L) in DMSO as a function of time in 100 mL of concentrated ammonia–water. (d) CIE gamut diagram corresponding to (c).

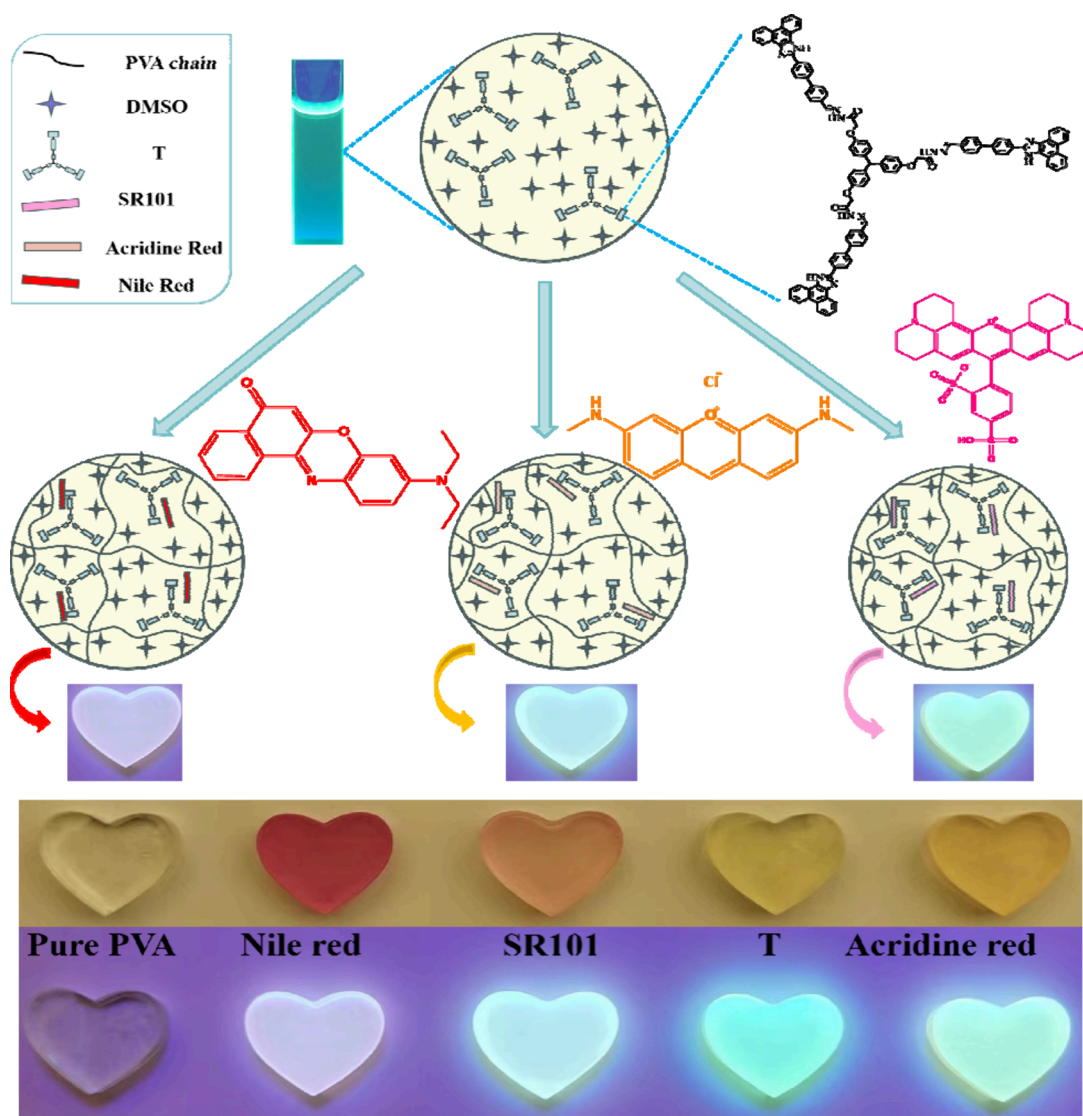
was gradually added to the solution with molecule T, the fluorescence intensity of molecule T at 476 nm reduced and a new emission band appeared at 570 nm. At the same time, it was observed that the fluorescence intensity of Acridine Red gradually increased. When the molar ratio of molecule T/Acridine Red was 20:1, the fluorescence intensity was the maximum in all measured data. The FRET process could be observed by comparing the fluorescence emission curves of molecule T/Acridine Red (20:1) and pure Acridine Red. Under 431 nm excitation, the fluorescence intensity of pure Acridine Red was low, and hence the increased amount of Acridine Red did not result in enhanced fluorescence intensity of the dye (Figure 4a). Further, the enhanced fluorescence intensity of Acridine Red at 570 nm is due to the transfer of energy from molecule T to Acridine Red. To quantitatively evaluate the ALHS, we calculated the energy transfer efficiency to be 9.44%. In addition, the fluorescence quantum yield of the

ALHS was 68.9% and the fluorescence lifetime was  $\tau = 2.17$  ns in the luminescence range from 450 to 860 nm. At the same concentration of T molecules, the fluorescence quantum yield of pure T molecule DMSO solution is 71.47% and the fluorescence lifetime is  $\tau = 2.41$  ns (Figures S16 and S17). By comparing the fluorescence lifetimes of T and T–Acridine Red, it can be observed that the fluorescence lifetime of T–Acridine Red is reduced by 0.24 ns compared to T, indicating the transfer of energy from the donor T to the acceptor Acridine Red. Similarly, this assertion can be validated by contrasting the fluorescence lifetime  $\tau = 0.98$  ns and fluorescence quantum yield 56.51% of the T–Nile Red DMSO solution with the fluorescence lifetime  $\tau = 0.9$  ns and fluorescence quantum yield 60.17% of the T–SR101 DMSO solution. Both sets of values are substantially lower than those of the pure T DMSO solution. The corresponding fluorescence data for Nile Red and SR101 are provided in Figures S18 and S19 and Table S1. The energy transfer efficiency of the ALHS based on T/Nile Red is 23.72% (molecule T/Nile Red = 20:1), and the emission color coordinate was calculated to be (0.33, 0.25). Meanwhile, the energy transfer efficiency of the ALHS based on T/SR101 is 9.74% (molecule T/SR101 = 50:1), and the emission color coordinate was calculated to be (0.32, 0.33).

The solutions' potential application as alkaline gas sensing materials was also evaluated. After the reaction between molecule T and alkaline substances, the deprotonation of phenanthroimidazole hydrogen in molecule T leads to fluorescence quenching of molecule T, which can be used as a means of detecting alkaline gas leakage. From the fluorescence spectra of the interaction between the DMSO solution of T and various alkaline substances, it can be seen that (Figure S20), under UV irradiation (431 nm), substances that are more basic than ammonia–water can completely quench the fluorescence of molecule T (Figure S21). We placed DMSO solution containing T molecules and ammonia solution in the same enclosed space and observed a rapid decrease in fluorescence intensity of the DMSO solution containing T, and the fluorescence color changed from cyan light to orange light (Figures 4c and 4d). At 15 min, the fluorescence intensity was greatly decreased and almost completely quenched after 1 h.

Previous studies have shown that not all supramolecular compounds are capable of self-assembling to form gels.<sup>31–33</sup> Additionally, the molecule that we synthesized, molecule T, is a type that fails to self-assemble into a gel, limiting its practical application. To better use the light-capture system based on molecule T in practice, we used PVA as a carrier to prepare a fluorescent gel based on the ACQ effect. By adding different dyes Acridine Red, SR101 and Nile Red to the PVA/T gel system, the fluorescence color of the PVA/T gel system changes. Under UV irradiation, the PVA/T gel emitted cyan fluorescence, while the PVA/T–SR101, PVA/T–Nile Red, and PVA/T–Acridine Red gels fluoresce cool white, warm white, and cyan white, respectively. (Scheme 2). The prepared gel sample was removed from the glass Petri dish and cut into thin strips, and its mechanical properties were evaluated by artificial deformation and tensile tests. As shown in Figures S22 and S23 and Table S2, the PVA/T–Nile Red gel has withstood significant mechanical deformation tests, including tensile deformation and deformation/tension, with no obvious cracks or fractures observed. The PVA/T–Nile Red gel showed significant elongation ( $\sim 685\%$ ) and tensile strength (516.88

Scheme 2. Schematic of the Light-Capture System Loaded on a PVA Gel and Images of the Pure PVA Gel and T–Nile Red, T–SR101, Molecule T, and T–Acridine Red Loaded onto PVA Gel under Natural and UV Light (365 nm)<sup>a</sup>



<sup>a</sup>Inset: images under UV irradiation (365 nm).

KPa), and its strain–stress data are the best among the three white light gels. At the same time, under the 430 nm ultraviolet light, although the white light brightness of the PVA/T–Nile Red gel is the lowest among the three white light gels, the white light chromicity coordinate (0.29, 0.33) emitted by the PVA/T–Nile Red gel is the closest to pure white light among the three white fluorescent gels, so we focus on the performance of the PVA/T–Nile Red gel. The PVA/T–Nile Red gel has certain recyclability. After five thermoplastic processes, the PVA/T–Nile Red gel has little mass loss, which indicates that the gel has good recyclability. However, it should be noted that with the increase of the thermoplastic times of the PVA/T–Nile Red gel, its fluorescent color will shift from white light to blue and white light. This may be because with the increase of the thermoplastic times, a part of the Nile Red dye loaded in the gel is decomposed at high temperature, resulting in the reduction of the red light component of the PVA/T–Nile Red gel (Figure S24). In addition, the four fluorescent gels can form different shapes through plastic deformation (Figure S25).

Prepared gel was prepared as a writing material. The interaction between  $\text{Fe}^{3+}$  and PVA/molecule T gel enables the use of the gel as a writing material and achieves information protection to a certain extent. As shown in the fluorescence spectrum (Figure S26), under UV irradiation (431 nm),  $\text{Fe}^{3+}$  was able to quench the fluorescence of the DMSO solution with molecule T. We speculate that this phenomenon is due to paramagnetic quenching caused by the coordination between the empty orbitals of  $\text{Fe}^{3+}$  and the lone pair electrons of nitrogen atoms in molecule T.<sup>34</sup> Interestingly, when an aqueous  $\text{Fe}^{3+}$  solution was applied on the PVA/T gel (Figure S27), significant fluorescence quenching was observed under UV irradiation (365 nm). At the same time, lighter writing traces were seen in natural light. Therefore, the PVA/molecule T gel can be used as a writing material for achieving information protection.

## CONCLUSIONS

In summary, we designed and synthesized a cyan-light-emitting three-arm molecule T, and the FRET process from donor (T)

to acceptor (Acridine Red, SR101, and Nile Red) was predicted by theoretical calculations. Based on the calculation results, three ALHSs were successfully constructed by mixing molecule T with a fluorescent dye (Acridine Red, SR101, and Nile Red). The three ALHSs were loaded on PVA to prepare fluorescent gels with white fluorescence; the prepared gels showed light transmission capability, high tensile strength, and thermal reshaping characteristics, and the gels can also be used as a writing material for achieving information protection and as an alkaline gas detection material. This study provides a basis for the design and manufacture of ALHSs based on multiperformance fluorescent gels.

## ■ ASSOCIATED CONTENT

### SI Supporting Information

The Supporting Information is available free of charge at <https://pubs.acs.org/doi/10.1021/acsaoam.4c00219>.

Optimization of the ground-state structure for the T molecule; UV absorption spectra; fluorescence spectra; synthetic route of molecule T;  $^1\text{H}$  NMR spectra and  $^{13}\text{C}$  NMR spectra;  $^1\text{H}$  NMR concentration spectra; EI-MS spectra; pictures of fluorescence quantum yield; fluorescence lifetimes; gel tensile diagram and gel stress-strain curve diagram; photograph of gel recyclability; graph of mass change during gel recyclability process; gel plasticity photograph; and photograph of gel-based writing material (PDF)

## ■ AUTHOR INFORMATION

### Corresponding Authors

**Xinxian Ma** – Ningxia Key Laboratory of Green Catalytic Materials and Technology, College of Chemistry and Chemical Engineering, Ningxia Normal University, College of Chemistry and Chemical Engineering, Ningxia Normal University, Guyuan 756099, China; [orcid.org/0000-0001-6977-1346](https://orcid.org/0000-0001-6977-1346); Email: [maxinxian@163.com](mailto:maxinxian@163.com)

**Shixun Lian** – Ningxia Key Laboratory of Green Catalytic Materials and Technology, College of Chemistry and Chemical Engineering, Ningxia Normal University, College of Chemistry and Chemical Engineering, Ningxia Normal University, Guyuan 756099, China; Key Laboratory of Light-Energy Conversion Materials of Hunan Province College, College of Chemistry and Chemical Engineering, Hunan Normal University, Changsha, Hunan 410081, People's Republic of China; [orcid.org/0000-0001-6524-2703](https://orcid.org/0000-0001-6524-2703); Email: [slxian@hunnu.edu.cn](mailto:slxian@hunnu.edu.cn)

**Yun Yan** – Ningxia Key Laboratory of Green Catalytic Materials and Technology, College of Chemistry and Chemical Engineering, Ningxia Normal University, College of Chemistry and Chemical Engineering, Ningxia Normal University, Guyuan 756099, China; Beijing National Laboratory for Molecular Sciences (BNLMS), College of Chemistry and Molecular Engineering, Peking University, Beijing 100871, China; [orcid.org/0000-0001-8759-3918](https://orcid.org/0000-0001-8759-3918); Email: [yunyan@pku.edu.cn](mailto:yunyan@pku.edu.cn)

### Authors

**Yuehua Liang** – Ningxia Key Laboratory of Green Catalytic Materials and Technology, College of Chemistry and Chemical Engineering, Ningxia Normal University, College of Chemistry and Chemical Engineering, Ningxia Normal University, Guyuan 756099, China

**Jiuzhi Wei** – Ningxia Key Laboratory of Green Catalytic Materials and Technology, College of Chemistry and Chemical Engineering, Ningxia Normal University, College of Chemistry and Chemical Engineering, Ningxia Normal University, Guyuan 756099, China

**Juan Zhang** – Ningxia Key Laboratory of Green Catalytic Materials and Technology, College of Chemistry and Chemical Engineering, Ningxia Normal University, College of Chemistry and Chemical Engineering, Ningxia Normal University, Guyuan 756099, China

**Enke Feng** – Ningxia Key Laboratory of Green Catalytic Materials and Technology, College of Chemistry and Chemical Engineering, Ningxia Normal University, College of Chemistry and Chemical Engineering, Ningxia Normal University, Guyuan 756099, China; [orcid.org/0000-0002-6367-0074](https://orcid.org/0000-0002-6367-0074)

**Zhenxing Fu** – Ningxia Key Laboratory of Green Catalytic Materials and Technology, College of Chemistry and Chemical Engineering, Ningxia Normal University, College of Chemistry and Chemical Engineering, Ningxia Normal University, Guyuan 756099, China

Complete contact information is available at: <https://pubs.acs.org/10.1021/acsaoam.4c00219>

### Author Contributions

$\nabla$ X.M.: conceptualization, resources, funding acquisition, and writing—review and editing. Y.L.: methodology, investigation, and writing—original draft. J.W.: materials characterization and performance tests. J.Z., S.L., Y.Y., E.F., and Z.F.: performance tests. X.M. and Y.L. contributed equally to this work. They should thus be considered co-first authors.

### Notes

The authors declare no competing financial interest.

## ■ ACKNOWLEDGMENTS

This work was supported by the National Natural Science Foundation of China (21961029), the Key Laboratory of Green Catalytic Materials and Technology of Ningxia (ZDSY03), and the Natural Science Foundation of Ningxia, China (2022AAC03337), all of which are gratefully acknowledged.

## ■ REFERENCES

- (1) Hu, Y.-X.; Jia, P.-P.; Zhang, C.-W.; Xu, X.-D.; Niu, Y.; Zhao, X.; Xu, Q.; Xu, L.; Yang, H.-B. A supramolecular dual-donor artificial light-harvesting system with efficient visible light-harvesting capacity. *Organic Chemistry Frontiers* **2021**, *8* (19), 5250–5257.
- (2) Yan, S.; Gao, Z.; Yan, H.; Niu, F.; Zhang, Z. Combination of aggregation-induced emission and clusterization-triggered emission in mesoporous silica nanoparticles for the construction of an efficient artificial light-harvesting system. *Journal of Materials Chemistry C* **2020**, *8* (41), 14587–14594.
- (3) Cao, X.; Li, Y.; Zhang, X.; Gao, A.; Xu, R.; Yu, Y.; Hei, X. Surface wettability and emission behavior tuned via solvent in a supramolecular self-assembly system based on a naphthalene diimides derivative. *Appl. Surf. Sci.* **2020**, *501*, 144256.
- (4) Zhao, Q.; Dai, X.-Y.; Yao, H.; Zhang, Y.-M.; Qu, W.-J.; Lin, Q.; Wei, T.-B. Stimuli-responsive supramolecular hydrogel with white AIE effect for ultrasensitive detection of Fe<sup>3+</sup> and as rewritable fluorescent materials. *Dyes Pigm.* **2021**, *184*, 108875.
- (5) Ma, Y.; Wang, Q.; Deng, J.; Yan, X.; Liu, J.; Ding, L.; Miao, R.; Fang, Y. Ultrabright Acrylic Polymers with Tunable Fluorescence

Enabled by Imprisoning Single TICT Probe. *Macromol. Rapid Commun.* **2024**, *45* (5), No. e2300592.

(6) Peng, Y.; Feng, Y.; Deng, G.-J.; He, Y.-M.; Fan, Q.-H. From Weakness to Strength: C–H/ $\pi$ -Interaction-Guided Self-Assembly and Gelation of Poly(benzyl ether) Dendrimers. *Langmuir* **2016**, *32* (36), 9313–9320.

(7) Yu, S. B.; Lin, F.; Tian, J.; Liu, Y.; Zhang, D. W.; Li, Z. T. Two-Dimensional Covalent and Supramolecular Polymers: From Monolayer to Bilayer and the Thicker. *Chemistry – A European Journal* **2022**, *28* (36), No. e202200914.

(8) Cheng, Q.; Cao, Z.; Hao, A.; Zhao, Y.; Xing, P. Fluorescent Imprintable Hydrogels via Organic/Inorganic Supramolecular Coassembly. *ACS Appl. Mater. Interfaces* **2020**, *12* (13), 15491–15499.

(9) Abbel, R.; van der Weegen, R.; Pisula, W.; Surin, M.; Leclère, P.; Lazzaroni, R.; Meijer, E. W.; Schenning, A. P. H. J. Multicolour Self-Assembled Fluorene Co-Oligomers: From Molecules to the Solid State via White-Light-Emitting Organogels. *Chemistry – A European Journal* **2009**, *15* (38), 9737–9746.

(10) El-Khouly, M. E.; Kobaisy, A. M.; Sallam, G.; Yoshihisa, M. Intra-supramolecular electron transfer of the light harvesting porphyrin–phthalocyanine complex in aqueous medium. *J. Porphyrins Phthalocyanines* **2022**, *26* (02), 132–139.

(11) Ren, D.; Tang, L.; Wu, Z.; Zhang, Q.; Xiao, T.; Elmes, R. B. P.; Wang, L. An amphiphilic molecule with a single fluorophore exhibits multiple stimuli-responsive behavior. *Chin. Chem. Lett.* **2023**, *34* (11), 108617.

(12) Tang, L.; Wu, Z.; Zhang, Q.; Hu, Q.; Dang, X.; Cui, F.; Tang, L.; Xiao, T. A sequential light-harvesting system with thermosensitive colorimetric emission in both aqueous solution and hydrogel. *Chem. Commun.* **2024**, *60* (35), 4719–4722.

(13) Dai, X.-Y.; Huo, M.; Liu, Y. Phosphorescence resonance energy transfer from purely organic supramolecular assembly. *Nature Reviews Chemistry* **2023**, *7* (12), 854–874.

(14) Wang, Y.; Lai, Y.; Ren, T.; Tang, J.; Gao, Y.; Geng, Y.; Zhang, J.; Ma, X. Construction of Artificial Light-Harvesting Systems Based on Aggregation-Induced Emission Type Supramolecular Self-Assembly Metallogels. *Langmuir* **2023**, *39* (3), 1103–1110.

(15) Gu, M. J.; Han, X. N.; Guo, W. C.; Han, Y.; Chen, C. F. Naphth[4]arene: Synthesis, Conformations, and Application in Color-Tunable Supramolecular Crystalline Assemblies. *Angew. Chem., Int. Ed.* **2023**, *62* (42), No. e202305214.

(16) Li, D.; Wang, J.; Ma, X. White-Light-Emitting Materials Constructed from Supramolecular Approaches. *Advanced Optical Materials* **2018**, *6* (20), 1800273.

(17) Li, Y.; Dong, Y.; Cheng, L.; Qin, C.; Nian, H.; Zhang, H.; Yu, Y.; Cao, L. Aggregation-Induced Emission and Light-Harvesting Function of Tetraphenylethene-Based Tetracationic Dicyclopentane. *J. Am. Chem. Soc.* **2019**, *141* (21), 8412–8415.

(18) Han, S.; Shi, Y. Photonic crystal nanobeam/micro-ring hybrid-cavities for optical trapping. *Opt. Commun.* **2020**, *459*, 124902.

(19) Ding, J.-D.; Chen, J.-F.; Lin, Q.; Yao, H.; Zhang, Y.-M.; Wei, T.-B. A multi-stimuli responsive metallosupramolecular polypseudorotaxane gel constructed by self-assembly of a pillar[5]arene-based pseudo[3]rotaxane via zinc ion coordination and its application for highly sensitive fluorescence recognition of metal ions. *Polym. Chem.* **2018**, *9* (44), 5370–5376.

(20) Otomo, K.; Dewa, T.; Matsushita, M.; Fujiyoshi, S. Cryogenic Single-Molecule Fluorescence Detection of the Mid-Infrared Response of an Intrinsic Pigment in a Light-Harvesting Complex. *J. Phys. Chem. B* **2023**, *127* (22), 4959–4965.

(21) Bairi, P.; Roy, B.; Chakraborty, P.; Nandi, A. K. Co-assembled White-Light-Emitting Hydrogel of Melamine. *ACS Appl. Mater. Interfaces* **2013**, *5* (12), 5478–5485.

(22) Xiao, T.; Li, X.; Zhang, L.; Diao, K.; Li, Z.-Y.; Sun, X.-Q.; Wang, L. Artificial stepwise light harvesting system in water constructed by quadruple hydrogen bonding supramolecular polymeric nanoparticles. *Chin. Chem. Lett.* **2024**, *35* (2), 108618.

(23) Chen, W.-C.; Yuan, Y.; Ni, S.-F.; Tong, Q.-X.; Wong, F.-L.; Lee, C.-S. Achieving efficient violet-blue electroluminescence with

CIEy < 0.06 and EQE > 6% from naphthyl-linked phenanthroimidazole–carbazole hybrid fluorophores. *Chemical Science* **2017**, *8* (5), 3599–3608.

(24) Barot, Y. B.; Anand, V.; Mishra, R. White light emission from fluorescent ionic liquids in the solution and gel forms using RGB system. *J. Photochem. Photobiol., A* **2024**, *446*, 115109.

(25) Ma, C.; Wang, Y.; Han, N.; Zhang, R.; Liu, H.; Sun, X.; Xing, L. Carbon dot-based artificial light-harvesting systems with sequential energy transfer and white light emission for photocatalysis. *Chin. Chem. Lett.* **2024**, *35* (4), 108632.

(26) Song, B.; Zhang, L.; Sun, J.; Lam, J. W. Y.; Tang, B. Z. In Situ Synthesis of AIEgen-based Porous Organic Polymer Films by Interfacial Amino-yne Click Polymerization for Efficient Light-Harvesting. *Angew. Chem., Int. Ed.* **2023**, *62* (18), No. e202302543.

(27) Guo, S.; Song, Y.; He, Y.; Hu, X. Y.; Wang, L. Highly Efficient Artificial Light-Harvesting Systems Constructed in Aqueous Solution Based on Supramolecular Self-Assembly. *Angew. Chem., Int. Ed.* **2018**, *57* (12), 3163–3167.

(28) Xiao, T.; Wu, H.; Sun, G.; Diao, K.; Wei, X.; Li, Z.-Y.; Sun, X.-Q.; Wang, L. An efficient artificial light-harvesting system with tunable emission in water constructed from a H-bonded AIE supramolecular polymer and Nile Red. *Chem. Commun.* **2020**, *56* (80), 12021–12024.

(29) Humphrey, W.; Dalke, A.; Schulten, K. VMD: Visual molecular dynamics.pdf. *J. Mol. Graphics* **1996**, *14* (1), 33–38.

(30) Lu, T.; Chen, F. Multiwfn: A multifunctional wavefunction analyzer. *J. Comput. Chem.* **2012**, *33* (5), 580–592.

(31) Euti, E. M.; Wolfel, A.; Picchio, M. L.; Romero, M. R.; Martinelli, M.; Minari, R. J.; Igarzabal, C. I. A. Controlled Thermoreversible Formation of Supramolecular Hydrogels Based on Poly(vinyl alcohol) and Natural Phenolic Compounds. *Macromol. Rapid Commun.* **2019**, *40* (18), 1900217.

(32) Wolfel, A.; Euti, E. M.; Picchio, M. L.; Romero, M. R.; Galván Josa, V. M.; Martinelli, M.; Minari, R. J.; Alvarez Igarzabal, C. I. Unraveling the gallol-driven assembly mechanism of thermoreversible supramolecular hydrogels inspired by ascidians. *Polym. Chem.* **2020**, *11* (45), 7185–7198.

(33) Li, W.; Zeng, X.; Wang, H.; Wang, Q.; Yang, Y. PVA-reinforced glutathione–Ag hydrogels and release of Ag nanoparticles and drugs by UV-triggered controllable disassembly. *New J. Chem.* **2016**, *40* (5), 4528–4533.

(34) Tang, X.; Wang, Y.; Han, J.; Ni, L.; Wang, L.; Li, L.; Zhang, H.; Li, C.; Li, J.; Li, H. A relay identification fluorescence probe for Fe<sup>3+</sup> and phosphate anion and its applications. *Spectrochimica Acta Part A: Molecular and Biomolecular Spectroscopy* **2018**, *191*, 172–179.